# Model of a two-dimensional Fermi liquid

H. V. da Silveira*
*Department of Physics and Astronomy, Northwestern University, Evanston, Illinois 60208*

Marcos H. Degani
*Instituto de Física e Química de São Carlos, Universidade de São Paulo, 13560 São Carlos, SP, Brazil*

K. S. Singwi†
*Department of Physics and Astronomy, Northwestern University, Evanston, Illinois 60208*
(Received 17 December 1991)

In this paper we use a self-consistent scheme proposed by Singwi, Tosi, Land, and Sjölander to study a two-dimensional Fermi liquid whose particles interact via a repulsive hard-core potential with or without an attractive tail. We determine the Landau parameters $F_0^s$ and $F_0^a$, the static structure factors, and we discuss the effect of adding the attractive tail to the hard-core potential.

## I. INTRODUCTION

In 1987 Ng and Singwi[1] presented a detailed microscopic study of a model system of a Fermi liquid whose particles interact via a repulsive hard-core potential and an attractive tail. The model is constructed to simulate $^3$He. The study is based on a self-consistent scheme of Singwi, Tosi, Land, and Sjölander[2] (STLS) that has been used to study correlations in electron liquids. This same scheme has been applied to study a fully polarized[3] and a partially polarized[4] model Fermi liquid. In Ref. 3 they have compared some of the properties of a polarized system with those of an unpolarized model Fermi liquid, and in Ref. 4 they have investigated the corresponding system of a partially polarized model Fermi liquid, which is a subject of experimental interest.[5]

In this paper we extend the same model and the theory to investigate the two-dimensional (2D) Fermi liquid; it was motivated by recent experiments involving 2D $^3$He adsorbed on graphite.[6–8] The theoretical scheme used in this paper is self-consistent and is dynamic in nature. The only input, as in 3D,[1] is the bare potential.

We introduce the density and spin response functions in the form of a generalized random-phase approximation (RPA). We examine the effect of adding an attractive tail on properties that we studied. We found interesting results concerning the role of the attractive interaction. for example, the Landau parameter $F_0^a$ increases compared with its values in the hard-core case. The structure factors for spin fluctuations are quite different compared with the hard-core case. The microscopic theory that we use to study the 2D Fermi liquid enables us to study separately the effects of the hard-core and attractive part of the bare potential.

The present paper is organized as follows: In Sec. II we present a theoretical scheme based on that of STLS. In Sec. III, we calculate the two most important Landau parameters, $F_0^s$ and $F_0^a$, for small densities and also the compressibility ratio $K/K_f$. In Sec. IV, we discuss the static structure factors $S(k)$ and $\tilde{S}(k)$. In Sec. V, we include an attractive tail.

## II. THEORETICAL SCHEME

In the STLS scheme, the wave vector and frequency-dependent density and spin response function are written in the form[1]

$$\chi_d(k,\omega)=\frac{\chi_0(k,\omega)}{1-V^s_{\rm eff}(k,\omega)\chi_0(k,\omega)} \tag{1a}$$

and

$$\chi_s(k,\omega)=\frac{\mu_B^2\chi_0(k,\omega)}{1-V^a_{\rm eff}(k,\omega)\chi_0(k,\omega)}\ , \tag{1b}$$

where $\chi_d$ and $\chi_s$ are, respectively, the density and spin response functions, and $\chi_0$ is the Lindhard function. $V^s_{\rm eff}$ and $V^a_{\rm eff}$ are, respectively, the effective spin-symmetric and spin-antisymmetric particle-hole interactions, and $\mu_B$ is the Bohr magneton. The above equations are in the form of a generalized random-phase approximation (RPA).

Within the STLS scheme the effective interactions $V^s_{\rm eff}$ and $V^a_{\rm eff}$ considered static,[9] are written in terms of pair distribution functions in the form

$$V^s_{\rm eff}(r)=-\int_r^\infty dr\, g(r)\frac{dV(r)}{dr} \tag{2a}$$

and

$$V^a_{\rm eff}(r)=-\int_r^\infty dr\, \tilde{g}(r)\frac{dV(r)}{dr}\ , \tag{2b}$$

where $g(r)=g_{\uparrow\uparrow}(r)+g_{\uparrow\downarrow}(r)$ is the pair-correlation function and $\tilde{g}(r)=g_{\uparrow\uparrow}(r)-g_{\uparrow\downarrow}(r)$. $V(r)$ is the bare potential.

In the present case, we consider the bare potential in the form

 

$$V(r)=\begin{cases} V_0 , & r \le a_0 \\ 0 , & r > a_0 , \end{cases} \tag{3}$$

where $a_0$ is the hard-core radius and $V_0$ is positive. In the hard-core limit $V_0 \to \infty$. Substituting Eq. (3) into Eqs. (2a) and (2b), and taking the Fourier transform of $V^s_{\text{eff}}(r)$ and $V^a_{\text{eff}}(r)$, we obtain

$$V^s_{\text{eff}}(k)=\frac{2\pi V_0 g(a_0) a_0}{k} J_1(ka_0) \tag{4}$$

and a similar expression for $V^a_{\text{eff}}(k)$, with $g(a_0)$ replaced by $\tilde{g}(a_0)$. In Eq. (4), $J_1(ka_0)$ is the first-order Bessel function of the first kind.

The numbers $g(a_0)$ and $\tilde{g}(a_0)$ are obtained through pair-correlation functions $g(r)$ and $\tilde{g}(r)$, which are given by the inverse Fourier transform of the structure factor,

$$g(r)=1+\frac{1}{k_F^2}\int_0^\infty dk\, kJ_0(kr)[S(k)-1] \tag{5a}$$

and

$$\tilde{g}(r)=\frac{1}{k_F^2}\int_0^\infty dk\, kJ_0(kr)[\tilde{S}(k)-1] , \tag{5b}$$

where $J_0(ka_0)$ is the zeroth-order Bessel function of the first kind.

Using the fluctuation-dissipation theorem, we can write the static structure factor and the magnetic structure factor $\tilde{S}(k)$ in terms of the density and spin response functions $\chi_d$ and $\chi_s$, respectively, through

$$S(k)=-\frac{2}{k_F^2}\int_0^\infty d\omega\, \text{Im}\chi_d(k,\omega) \tag{6a}$$

and

$$\tilde{S}(k)=-\frac{2}{k_F^2}\int_0 d\omega\, \text{Im}\chi_s(k,\omega) . \tag{6b}$$

At $r=a_0$, we have to solve self-consistently the set of equations given by Eqs. (1), (4), (5), and (6) for $g(a_0)$ and $\tilde{g}(a_0)$.

The expression for the Lindhard function $\chi_0$ derived by Stern[10] is not convenient to use in Eq. (6). To calculate the structure factor $S(k)$ and all the other physical quantities mentioned, we follow instead a procedure used by de Freitas, Ioriatti, and Studart.[11] They replaced $k$ and $\omega$ by variables $\xi$ and $\theta$ defined by

$$\frac{2k_F}{k}=\cosh\xi \sin\theta , \tag{7a}$$

$$\frac{2m\omega}{\hbar k^2}=\sinh\xi \cos\theta , \tag{7b}$$

where $0<\theta<\pi/2$, $0\le\xi\le\infty$. With this transformation, the expression for $\chi_0(k,\omega)$ assumes the form

$$\chi_0(\theta)=-(m/\pi\hbar^2)(1-\cos\theta) . \tag{8}$$

Using Eqs. (1) and (8) in Eq. (6) and writing $k$ in units of the Fermi wave vector $k_F$, the structure factor $S(k)$ becomes

$$S(k)=\frac{2k}{\pi}\int_0^{\alpha(k)} d\theta \left[\sqrt{1-(k^2/4)\sin^2\theta}+\frac{\cot^2\theta}{\sqrt{1-(k^2/4)\sin^2\theta}}\right]\times\left[\frac{(1-\cos\theta)}{1+V^s_{\text{eff}}(k)(m/\pi\hbar^2)(1-\cos\theta)}\right] , \tag{9}$$

where

$$\alpha(k)=\begin{cases} \pi/2 , & k \le 2 \\ \sin^{-1}(2/k) , & k > 2 . \end{cases} \tag{10}$$

The expression for $\tilde{S}(k)$ is similar, replacing $V^s_{\text{eff}}(k)$ with $V^a_{\text{eff}}(k)$.

Writing $x=V_0 g(a_0)$ in units of the Fermi energy, we have from Eq. (5),

$$F(x)=1+\int_0^\infty dk\, kJ_0(ka_0)[S(k,x)-1] , \tag{11a}$$

where

$$F(x)=x/V_0 .$$

In the hard-core limit ($V_0 \to \infty$), we expect $g(a_0)\to 0$. The effective interaction $V^s_{\text{eff}}(k;x)$ is determined by

$$F(x)=0 . \tag{11b}$$

In the case of the spin response, we write $y=V_0\tilde{g}(a_0)$ in units of the Fermi energy; and for the spin-antisymmetric effective interaction, we have to solve an

TABLE I. Solution of the STLS equation for various densities for a pure hard-core potential with $V_0 g(a_0)$ and $-V_0\tilde{g}(a_0)$ in units of the Fermi energy.

| $c(a_0k_F)$ | $n/n_0$ | $V_0 g(a_0)$ | $-V_0\tilde{g}(a_0)$ |
|---|---|---|---|
| 0.1 | | 8.01 | 7.91 |
| 0.2 | | 5.5 | 5.46 |
| 0.3 | | 4.67 | 4.45 |
| 0.4 | | 4.35 | 3.75 |
| 0.5 | | 4.27 | 3.28 |
| 0.6 | | 5.11 | 4.40 |
| 0.7 | | 6.82 | 2.59 |
| 0.8 | | 14.72 | 2.35 |
| 0.9 | 0.405 | 28.53 | 2.12 |
| 1.0 | 0.500 | 45.05 | 1.84 |
| 1.1 | 0.605 | 67.22 | 1.59 |
| 1.2 | 0.720 | 60.17 | 1.40 |
| 1.3 | 0.845 | 46.64 | 1.23 |
| 1.4 | 0.980 | 35.99 | 1.09 |
| 1.41 | 1.0 | 34.83 | 1.07 |

equation of the form

$$y/V_0 = G(y) , \tag{12a}$$

where we can see that

$$G(y) = F(y) - 1 . \tag{12b}$$

We solved numerically Eqs. (11) and (12a) in the hard-core limit for various densities, below the critical value $a_0 k_F \approx 1.41$. Beyond this value the self-consistent solution does not exist and the system may solidify. Solutions for $g(a_0)$ and $\tilde{g}(a_0)$ so obtained are given in Table I for various densities.

## III. LANDAU PARAMETERS

In the region of density $a_0 k_F < 1$, we calculate the Landau parameters $F_0^s = N(0) V_{\text{eff}}^s(k=0)$ and $F_0^a = N(0) V_{\text{eff}}^a(k=0)$, where $N(0)$ is the density of states $N(0) = m/\pi\hbar^2$. Our results are shown in Fig. 1 in terms of $c = a_0 k_F$. In the limit of $c \to 0$, the spin and density Landau parameters reach the same absolute value. Due to the Pauli exclusion principle, the effective interaction between particles of the same spin vanishes. The compressibility ratio $K/K_f$, where $K_f$ is the free particle compressibility, is given by

$$\frac{K}{K_f} = \frac{1}{1+F_0^s} , \tag{13}$$

since $m^*/m = 1$. This ratio is shown in Fig. 2 as a function of $c$, and we can see that the curve is smooth as in 3D, but our values of $K/K_f$ are much smaller than those in 3D. The pair-correlation functions $g(r)$ and $\tilde{g}(r)$ for low densities are nonzero inside the hard core, although $g(a) = \tilde{g}(a_0) = 0$. This is a defect of this theory for large values of $k$. This behavior, as in 3D, may not be perceptible in a plot of $S(k)$ and $\tilde{S}(k)$, but can lead to unphysical behavior of the pair-correlation functions for small values of $r$.

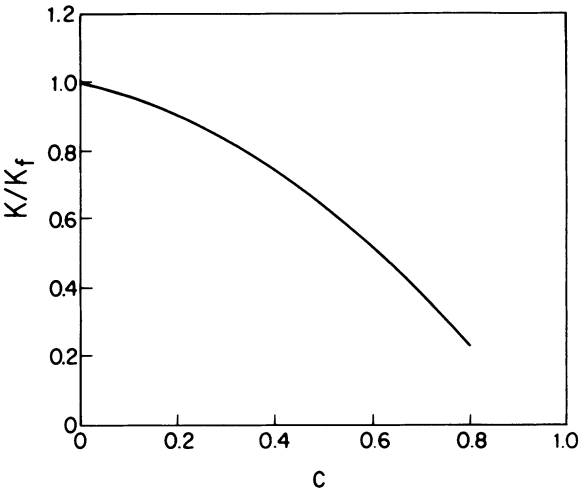


FIG. 2. Compressibility ratio $K/K_f$ vs $c$.

## IV. THE STATIC STRUCTURE FACTORS

The high-density region $c > 1$, as in 3D, is very interesting since the liquid $^3$He in a first approximation can be considered a Fermi liquid interacting via a hard-core potential. Taking $a_0 \approx 2.56$Å and $k_F \approx 0.55$Å$^{-1}$, corresponding to the normal liquid $^3$He density,[7-9] one finds that $c \approx 1.41$. However, the real liquid $^3$He interacts via softer potential with an attractive tail (6-12 Lennard-Jones potential), and we shall see that the appropriate value of $c$ for 2D $^3$He is $c \approx 0.9-1.1$.

The static structure factor $S(k)$ for densities $c = 1.0$, 1.1, and 1.2 is shown in Fig. 3. It can be seen that the peak positions for different concentrations all occur at around $ka_0 = 4.75$, and the peak value increases with the increase in density. In the 3D case,[1] similar results have

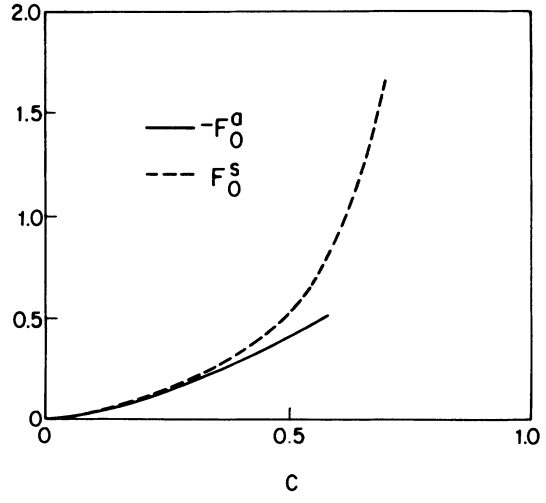


FIG. 1. Landau parameters $F_0^s$ and $-F_0^a$ vs $c$ for small densities.

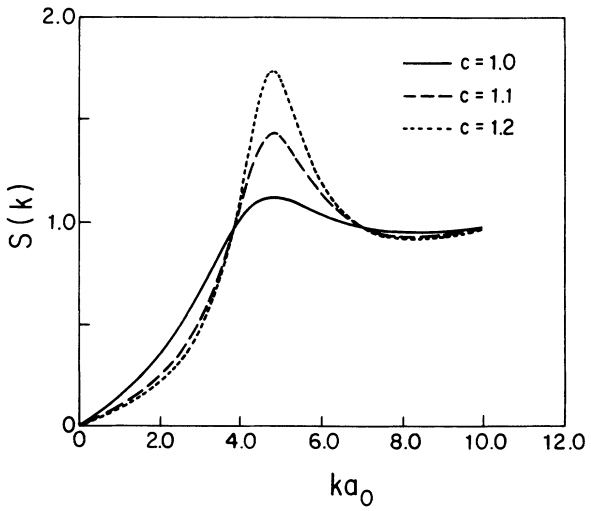


FIG. 3. Static structure factor $S(k)$ vs $ka_0$ for densities $c = 1.0$, 1.1, and 1.2 for a pure hard-core potential.

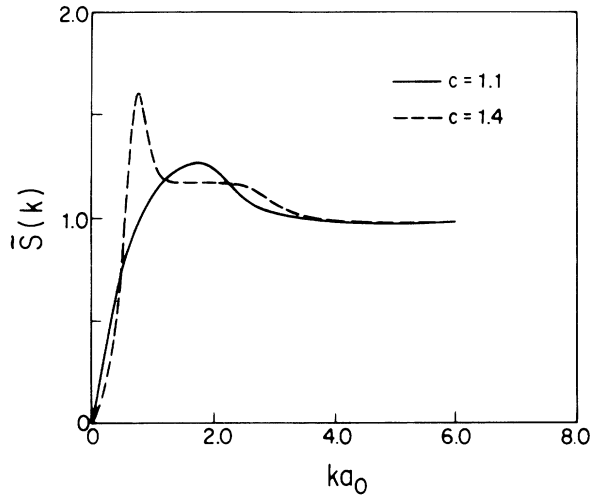


FIG. 4. Magnetic structure factor $\tilde{S}(k)$ vs $ka_0$ for densities $c=1.1$ and 1.4, for a pure hard-core potential.

been found.

The static magnetic structure factor $\tilde{S}(k)$ for densities $c=1.1$ and 1.4 is shown in Fig. 4. We can see the presence of a sharp spike for $c=1.4$. At this density, we have ferromagnetic instability since $F_0^a<-1$, and this is the reason for the appearance of this behavior in $\tilde{S}(k)$.

## V. INCLUSION OF AN ATTRACTIVE TAIL

The attractive tail has an important role in determining the properties of liquid $^3$He. In real liquid $^3$He, the interatomic potential is of the Lennard-Jones type, which has an attractive tail.

The model interaction has the form

$$V(r)=\begin{cases} V_0 \ (V_0\to\infty), & r<a_0 \ , \\ -\varepsilon, & a_0<r<a_1 \ , \\ 0, & a_1,<r \ . \end{cases} \tag{14}$$

This potential includes a repulsive hard core at short distances and a short-ranged attractive tail.

The parameter $a_1$ and $\varepsilon$ of the attractive tail are fixed in Ref. 1, to be $a_1=2.05a_0$ and $\varepsilon\approx 0.46\bar{\varepsilon}$, where $4\bar{\varepsilon}$ is the strength of the Lennard-Jones potential for $^3$He.

Using Eqs. (2) and (14) and taking the Fourier transform of $V^s_{\rm eff}(r)$ and $V^a_{\rm eff}(r)$ we obtain

$$V^s_{\rm eff}(k)=(2\pi/k)[(V_0+\varepsilon)g(a_0)J_1(ka_0) -\varepsilon a_1 g(a_1)J_1(ka_1)] \ , \tag{15}$$

and a similar expression for $V^a_{\rm eff}(k)$ replacing $g(a_0)$ with $\tilde{g}(a_0)$.

Therefore, we have a new set of self-consistent equations for the variables $x_1=(V_0+\varepsilon)g(a_0)$, $x_2=-\varepsilon g(a_1)$ and $y_1=(V_0+\varepsilon)\tilde{g}(a_0)$, $y_2=-\varepsilon\tilde{g}(a_1)$ in units of Fermi energy. We now have to solve numerically two coupled nonlinear equations of two variables. Using the same procedure as in Sec. II, we can write

TABLE II. Solution of the STLS equation for various densities for a pure hard core plus an attractive potential, expressed in units of the Fermi energy.

| $c(a_0k_F)$ | $V_0g(a_0)$ | $\varepsilon g(a_1)$ | $-V_0g(a_0)$ | $-\varepsilon g(a_1)$ |
|---|---|---|---|---|
| 0.90 | 29.173 | 0.972 | | |
| 0.94 | 30.884 | 1.000 | | |
| 1.00 | 43.495 | 0.995 | 1.240 | 0.324 |
| 1.10 | 65.660 | 0.734 | 1.291 | 0.186 |
| 1.20 | 50.056 | 0.627 | 1.210 | 0.131 |
| 1.30 | 44.723 | 0.610 | 1.291 | 0.135 |
| 1.40 | 35.067 | 0.602 | 1.050 | 0.081 |
| 1.41 | 33.935 | 0.597 | 1.087 | 0.089 |

$$\frac{x_1}{V_0+\varepsilon}=F_1(x_1,x_2) \ , \tag{16a}$$

$$\frac{x^2}{\varepsilon}=F_2(x_1,x_2) \ , \tag{16b}$$

where

$$\begin{aligned} F_1(x_1,x_2)&=g(a_0;x_1,x_2) \ , \\ F_2(x_1,x_2)&=g(a_1;x_1,x_2) \ , \end{aligned} \tag{17}$$

$$\frac{y_1}{V_0+\varepsilon}=G_1(y_1,y_2) \ , \tag{18a}$$

$$\frac{y_2}{V_0+\varepsilon}=G_2(y_1,y_2) \ , \tag{18b}$$

where

$$\begin{aligned} G_1(y_1,y_2)&=\tilde{g}(a_0;y_1,y_2) \ , \\ G_2(y_1,y_2)&=\tilde{g}(a_1;y_1,y_2) \ . \end{aligned} \tag{19}$$

In the hard-core limit ($V_0\to\infty$), we have

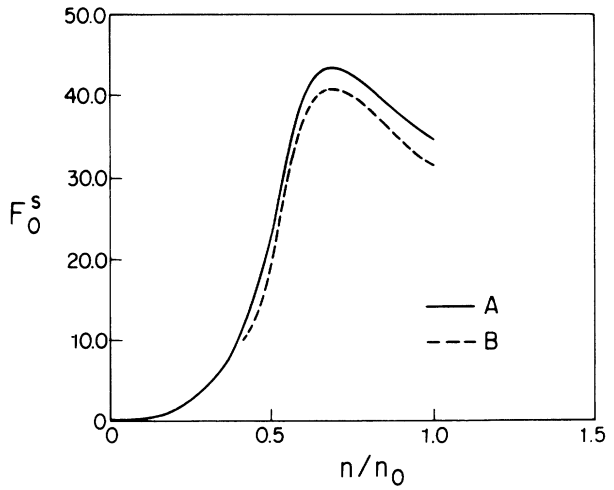


FIG. 5. Landau parameter $F_0^s$ vs $n/n_0$. Curve A is for a hard-core potential and curve B is for a hard-core plus an attractive tail potential.

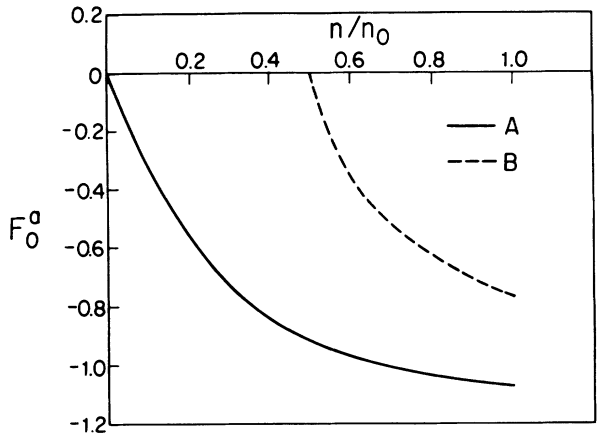


FIG. 6. Landau parameter $F_0^a$ vs $n/n_0$. Curve A is for a hard-core potential and curve B is for a hard core plus an attractive tail potential.

$$F_1(x_1,x_2)=0\ ,$$
$$F_2(x_1,x_2)-x_2/\varepsilon=0\ , \tag{20}$$

and a similar set of equations for the spin response.

The solutions of the above set of equations are given in Table II for differents densities $c$.

### A. Landau parameters

The Landau parameters $F_0^s$ and $F_0^a$ vs $n/n_0$ are shown in Figs. 5 and 6, respectively. Curve A is for a pure hard-core potential and curve B is for a hard core plus an attractive tail. Comparing the values of $F_0^s$ in curve A at $n/n_0=0.25$ and $n/n_0=0.50$, they differ by a factor of 19, whereas $F_0^a$ changes by 41.8%. Comparing curve A in Figs. 5 and 6, the Landau parameter $F_0^s$ changes more rapidly with density than $F_0^a$ in the region of high density,

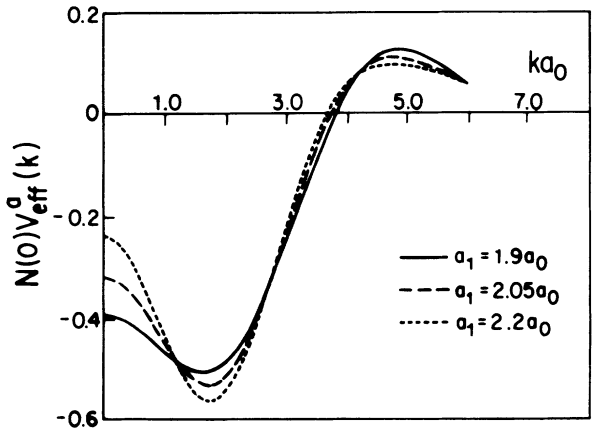


FIG. 7. Spin-antisymmetric dimensionless effective interaction $N(0)V_{\rm eff}^a(k)$ vs $ka_0$ for three different choices of the parameter $a_1$ (and $\varepsilon$) for the attractive tail, for density $c=1.1$.

$c>1$. Near the critical point $c\approx 1.41$, $F_0^s$ decreases. As in 3D, the present theory may not be valid when the system is close to its solidification point.

The inclusion of an attractive tail in $F_0^a$ has a large effect, as can be seen in Fig. 6. We also solved the self-consistent equations for two or more choices of the parameter $\varepsilon$ and $a_1$ for the density $c=1.1$. Note in Table III that the values of the effective spin-symmetric interaction $V_{\rm eff}^s(k)$ are very close for different values of $a_1$ in all ranges of $k$. The Landau parameters $F_0^s[N(0)V_{\rm eff}^s(k=0)]$ for three different choices of $a_1$ and $\varepsilon$ are very close. This situation is not the same for the effective spin-antisymmetric interaction $V_{\rm eff}^a(k)$ (Fig. 7). The Landau parameter $F_0^a[N(0)V_{\rm eff}^a(k=0)]$ depends on the shape of the potential. For three different choices of $a_1$ and $\varepsilon$, $F_0^a$ changes from $-0.237$ to $-0.391$. Therefore, the effective spin-antisymmetric interaction $V_{\rm eff}^a(k)$ is sensitive to the shape of the attractive part of the bare potential.

In Fig. 8, we have $N(0)V_{\rm eff}^a(k)$ for a pure hard-core potential (curve A) and for a hard core plus an attractive tail for density $c=1.1$ (curve B). For $ka_0>2.25$ the values for $N(0)V_{\rm eff}^a(k)$ are very close, but in the small-$k$ region the attractive tail changes the shape of the effective potential. The Landau parameter $F_0^a$ increases by a factor of approximately 1.5 from its hard-core value.

In Fig. 9, we have the effective spin-symmetric dimen-

TABLE III. Spin-symmetric dimensionless effective interaction $N(0)V_{\rm eff}^s(k)$ vs $ka_0$ for density $c=1.1$, for three different choices of the parameter $a_1$.

| | $N(0)V_{\rm eff}^s(k)$ | | |
|---|---|---|---|
| $ka_0$ | $a_1=1.9a_0$ | $a_1=2.05a_0$ | $a_1=2.2a_0$ |
| 0.00 | 38.121 | 37.858 | 37.575 |
| 0.25 | 37.856 | 37.609 | 37.346 |
| 0.50 | 37.066 | 36.864 | 36.655 |
| 0.75 | 35.766 | 35.629 | 35.499 |
| 1.00 | 33.980 | 33.917 | 33.874 |
| 1.25 | 31.744 | 31.752 | 31.787 |
| 1.50 | 29.108 | 29.172 | 29.262 |
| 1.75 | 26.133 | 26.231 | 26.344 |
| 2.00 | 22.896 | 23.000 | 23.105 |
| 2.25 | 19.483 | 19.570 | 19.639 |
| 2.50 | 15.988 | 16.040 | 16.060 |
| 2.75 | 12.513 | 12.521 | 12.491 |
| 3.00 | 9.157 | 9.123 | 9.056 |
| 3.25 | 6.014 | 5.949 | 5.866 |
| 3.50 | 3.167 | 3.089 | 3.013 |
| 3.75 | 0.685 | 0.613 | 0.563 |
| 4.00 | −1.382 | −1.433 | −1.444 |
| 4.25 | −3.008 | −3.026 | −2.999 |
| 4.50 | −4.184 | −4.168 | −4.111 |
| 4.75 | −4.924 | −4.879 | −4.810 |
| 5.00 | −5.260 | −5.199 | −5.136 |
| 5.25 | −5.237 | −5.174 | −5.135 |
| 5.50 | −4.910 | −4.861 | −4.854 |
| 5.75 | −4.343 | −4.318 | −4.344 |
| 6.00 | −3.599 | −3.602 | −3.653 |

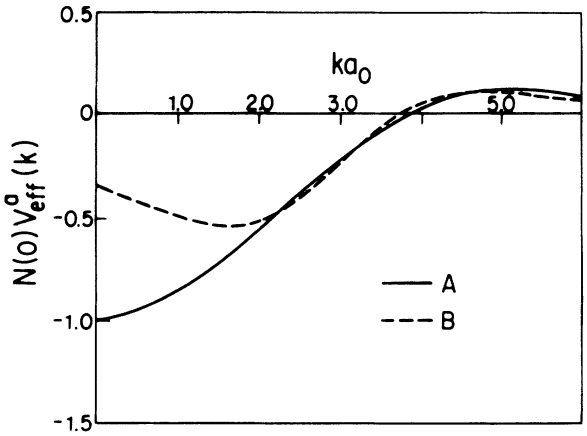


FIG. 8. Spin-antisymmetric dimensionless effective interaction $N(0)V^a_{\text{eff}}(k)$ vs $ka_0$ for $c=1.1$. Curve A is for a hard-core potential, and curve B for a hard-core plus an attractive tail potential.

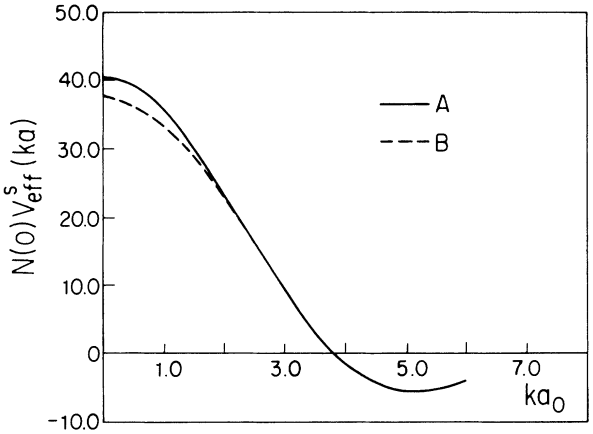


FIG. 9. Spin-symmetric dimensionless effective interaction $N(0)V^s_{\text{eff}}(k)$ vs $ka_0$ for $c=1.1$. Curve A is for a pure hard-core potential and curve B is for a hard-core plus an attractive tail potential.

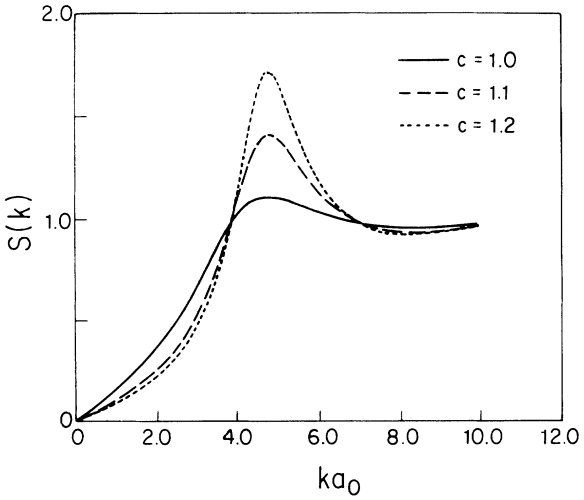


FIG. 10. The static structure factor $S(k)$ vs $ka_0$ for densities $c=1.0$, 1.1, and 1.2 for a hard-core plus an attractive tail potential.

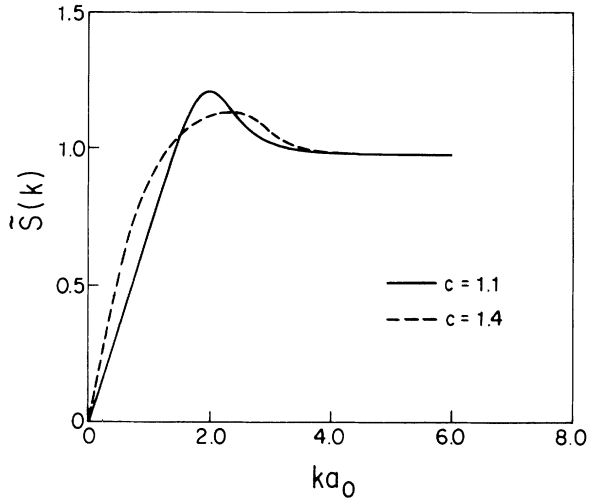


FIG. 11. Magnetic structure factor $\tilde{S}(k)$ vs $ka_0$ for densities $c=1.1$ and 1.4, for a hard-core plus an attractive tail.

sionless interaction $N(0)V^s_{\text{eff}}(k)$ for density $c=1.1$. Curve A is for a hard-core potential and curve B is for a hard core plus an attractive tail. Note that for small $k$, when we include an attractive tail, the effective potential decreases. But for $ka_0>2.25$, the values of the $N(0)V^s_{\text{eff}}(k)$ are very close.

### B. The static structure factor

The static structure factors $S(k)$ for densities $c=1.0$, 1.1, and 1.2 are shown in Fig. 10. Compared with the curves for $S(k)$ for a hard-core potential (Fig. 3), we can see that the peak position is the same and that the peak height increases with the density. This behavior has the same shape as in the 3D work of Ng and Singwi.[1]

The static magnetic structure factor $\tilde{S}(k)$ for densities $c=1.1$ and 1.4 are shown in Fig. 11. The shape of these curves is very different from the pure hard-core potential at the same densities. This is a consequence of the different behavior of the effective spin-antisymmetric interaction in the region of small $k$. Note that when the density increases, the peak of $\tilde{S}(k)$ weakens and in this situation the effect of the hard core becomes dominant.

The present study has provided us with some insight into the nature of the 2D liquid $He^3$. We also intend to determine the zero sound dispersion and the effective mass on the Fermi surface, although the former has a complicated analytical structure that is difficult to solve.

## ACKNOWLEDGMENTS

This work was supported by Conselho Nacional de Desenvolvimento Científico e Teconológico (CNPq). One of the authors (H.V.S.) is grateful to L. Liu and Tai Kai Ng for many valuable discussions and suggestions.

*Permanent address: Departamento de Física, Universidade Federal de São Carlos, 13560, SP, Brazil. Electronic mail address: UFSCARFC@BRFAPESP.BITNET.

†Deceased.

[1]Tai Kai Ng and K. S. Singwi, Phys. Rev. B **35**, 1708 (1987).

[2]K. S. Singwi, M. P. Tosi, R. Land, and A. Sjölander, Phys. Rev. **176**, 589 (1968).

[3]Tai Kai Ng and K. S. Singwi, Phys. Rev. Lett. **57**, 226 (1986).

[4]Tai Kai Ng and K. S. Singwi, Phys. Rev. B **35**, 6683 (1987).

[5]B. Casting and P. Nozièrez, J. Phys. (Paris) **40**, 257 (1979); see also A. Dutra and C. N. Archie, Phys. Rev. Lett. **55**, 2949 (1985).

[6]D. S. Greywall and P. A. Bush, Phys. Rev. Lett. **62**, 1868 (1989).

[7]D. S. Greywall, Phys. Rev. B **41**, 1842 (1990).

[8]D. S. Greywall and P. A. Bush, Phys. Rev. Lett. **65**, 64 (1990).

[9]K. S. Singwi and M. P. Tosi, in *Solid State Physics,* edited by H. Ehrenreich, F. Seitz, and D. Turnbull (Academic, New York, 1981), Vol. 36.

[10]F. Stern, Phys. Rev. Lett. **18**, 546 (1967).

[11]U. de Freitas, L. C. Ioriatti, and N. Studart, J. Phys. C **20**, 5983 (1987).